

Electronic Supporting Information

Development of benzylidene-methyloxazolone based AIEgens and decipherment of their working mechanism

Meijuan Jiang,^{ae} Zikai He,^{ab*} Yilin Zhang,^d Herman H.Y. Sung,^a Jacky W.Y. Lam,^{ae}
Qian Peng,^c Yongli Yan,^f Kam Sing Wong,^d Ian D. Williams,^a Yongsheng Zhao^f and
Ben Zhong Tang^{ae,g*}

^a Department of Chemistry, Hong Kong Branch of Chinese National Engineering Research Center for Tissue Restoration and Reconstruction, HKUST Jockey Club Institute for Advanced Study, Institute of Molecular Functional Materials, Division of Biomedical Engineering, State Key Laboratory of Molecular Neuroscience, Division of Life Science, Hong Kong University of Science and Technology, Clear Water Bay, Kowloon, Hong Kong. Email: tangbenz@ust.hk

^b School of Science, Harbin Institute of Technology, Shenzhen, 518055, China. Email: hezikai@hit.edu.cn

^c Key Laboratory of Organic Solids, Institute of Chemistry, Chinese Academy of Sciences, Beijing 100190, P.R. China.

^d Department of Physics, Hong Kong University of Science and Technology, Clear Water Bay, Kowloon, Hong Kong

^e HKUST-Shenzhen Research Institute, No. 9 Yuexing 1st RD, South Area, Hi-tech Park, Nanshan, Shenzhen 518057, China

^f Beijing National Laboratory for Molecular Sciences (BNLMS), Institute of Chemistry, Chinese Academy of Sciences, Beijing 100190, P.R. China

^g Guangdong Innovative Research Team, SCUT-HKUST Joint Research Laboratory, State Key Laboratory of Luminescent Materials and Devices, South China University of Technology, Guangzhou 510640, China

Author Contributions

M.J., Z.K. and B.Z.T conceived and designed the study. M.J. synthesized the compounds and performed characterizations. M.J., Y.Z. and K.S.W. performed the photophysical studies. H.H.Y.S. and I.D.W. performed the crystal structure analysis. M.J. and Q.P. performed and analyzed the theoretical calculations. Y.Y. and Y.Z. performed the waveguide experiments. M.J., Z.H., J.W.Y.L and B.Z.T. analyzed and discussed the results and prepared the manuscript.

Experimental Section

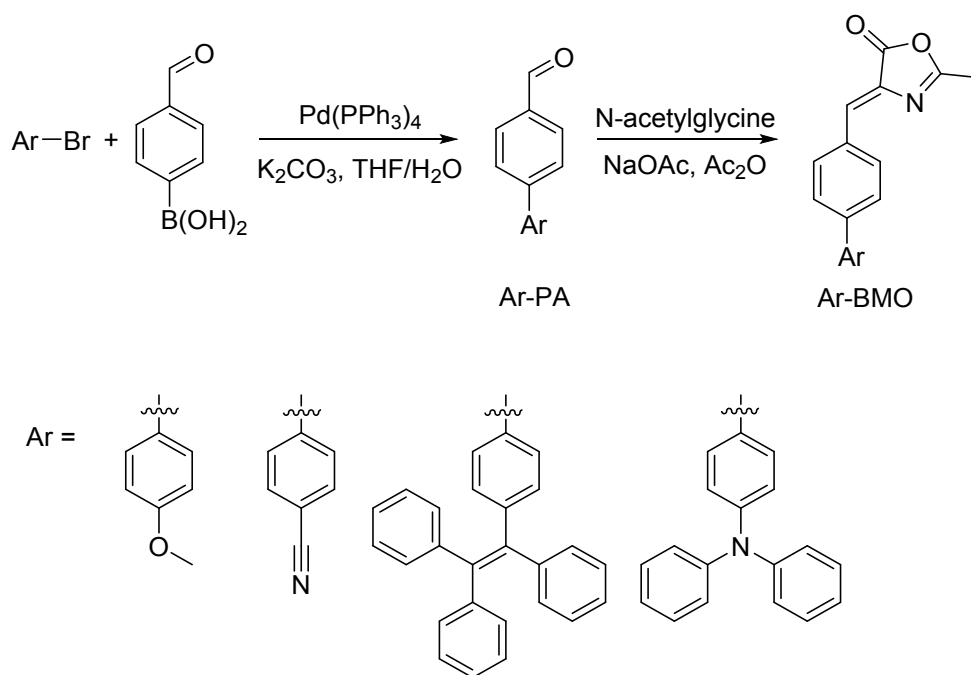
Materials and Instruments

Chemicals were purchased from J&K chemistry, Sigma-Aldrich and TCI and used directly without further purification. Tetrahydrofuran (THF) were distilled from sodium benzophenone ketyl under dry nitrogen immediately before use. Other solvents were directly used without further purification. ^1H and ^{13}C NMR spectra were recorded on a Bruker ARX 400 spectrometer using CDCl_3 as the solvent and tetramethyl silane(TMS) as the internal standard. High-resolution mass spectra (HRMS) were recorded on a GCT premier CAB048 mass spectrometer operated in a MALDI-TOF mode. UV-Vis absorption spectra were recorded on a Milton Roy Spectronic 3000 Array spectrometer. Photoluminescence spectra were recorded on a Perkin-Elmer LS 55 Spectrofluometer. The quantum yield values of solid and solutions were determined using an integrating sphere method, excited at 370 nm. Particle sizes were measured on a Zeta potential analyzer (Brookhaven, ZETAPLUS). The lifetime was measured by time-correlated single-photon counting method. Theoretical computations were carried out on the basis set of B3LYP/6-31G (d, p) by Gaussian 09.

Monitoring the *E/Z* isomerization

According to literature method,¹ 0.5 mL of BMOs solutions of CDCl_3 (40 mM or 20 mM) or d_6 -DMSO (20 mM) were prepared and added into the NMR tubes. After capping, the NMR tubes containing the solutions were placed under the irradiation of the same portable 365 nm UV mercury lamp at the same position. The process was monitored by NMR spectra at the interval of 5 min. The quantum yields of the photoisomerization from *Z*-isomer to *E*-isomer were calculated by the result of the first 5 min, in which the percentages of *E*-isomers were very small (< 10%).

Synthesis of BMOs



Scheme S1 Synthetic route for BMOs.

Briefly, using BMO-PH as an example, 4-biphenylaldehyde (364 mg, 2 mmol), N-acetylglycine (476 mg, 4 mmol), and NaOAc (164 mg, 2 mmol) in 5 mL acetic anhydride were heated in 120 °C oil bath for 3 h. After cooling to the room temperature, cold water was added and the mixture was extracted with dichloromethane. After removal of the solvent, the crude product was purified by silica gel column using hexane/ethyl acetate as eluent. Other compounds were synthesized similarly. The compounds were re-crystallized in dichloromethane/hexane before use. Single crystals for single crystal X-ray analysis were obtained in dichloromethane/hexane with slow layer-to-layer diffusion.

BMO-H, 47% yield. $^1\text{H NMR}$ (400 MHz, CDCl_3) δ (ppm) 8.09–8.07 (m, 2H), 7.47–7.43 (m, 3H), 7.15 (s, 1H), 2.42 (s, 3H). $^{13}\text{C NMR}$ (100 MHz, CDCl_3) δ (ppm) 168.0, 166.3, 133.3, 132.7, 132.4, 131.7, 131.3, 129.1, 15.9. MS (MALDI-TOF): calculated for $\text{C}_{11}\text{H}_9\text{NO}_2$ $[\text{M}+\text{H}]^+$ 188.0706, found 188.0714.

BMO-PH, 49.4% yield. $^1\text{H NMR}$ (400 MHz, CDCl_3) δ (ppm) 8.16 (d, 2H, $J = 8.4$ Hz), 7.69 (d, 2H, $J = 8.4$ Hz), 7.64 (d, 2H, $J = 7.2$ Hz), 7.49–7.46 (m, 2H), 7.41–7.40 (m, 1H), 7.19 (s, 1H), 2.43 (s, 3H). $^{13}\text{C NMR}$ (100 MHz, CDCl_3) δ (ppm) 168.0, 166.2, 143.9, 140.2, 132.9, 132.6, 132.3, 131.2, 129.2, 128.3, 127.7, 127.3, 15.9. MS (MALDI-TOF): calculated for $\text{C}_{17}\text{H}_{13}\text{NO}_2$ $[\text{M}+\text{H}]^+$ 264.1019, found 264.1022.

BMO-PF, 50.9% yield. $^1\text{H NMR}$ (400 MHz, CDCl_3) δ (ppm) 8.36 (s, 1H), 8.03(d, 2H, $J = 8.4$ Hz), 7.84 (d, 2H, $J = 8.0$ Hz), 7.58 (d, 2H, $J = 7.6$ Hz), 7.43–7.35 (m, 2H), 7.23 (s, 1H), 3.97 (s, 2H), 2.44 (s, 3H). $^{13}\text{C NMR}$ (100 MHz, CDCl_3) δ (ppm) 168.2, 165.8, 145.1, 144.6, 144.0, 140.9, 132.3, 132.1, 132.0, 131.9, 128.7, 128.1, 127.3, 125.5,

120.9, 120.4, 37.1, 15.9. MS (MALDI-TOF): calculated for C₁₈H₁₃NO₂ [M+H]⁺ 276.1025, found 276.1021.

BMO-PM, 50% yield. ¹H NMR (400 MHz, CDCl₃) δ (ppm) 8.13 (d, 2H, *J* = 8.4 Hz), 7.64 (d, 2H, *J* = 8.4 Hz), 7.59 (d, 2H, *J* = 6.4 Hz), 7.17 (s, 1H), 7.00 (d, 2H, *J* = 6.8 Hz), 3.86 (s, 3H), 2.42 (s, 3H). ¹³C NMR (100 MHz, CDCl₃) δ (ppm) 168.1, 166.0, 160.0, 143.5, 139.5, 132.9, 132.6, 132.3, 131.7, 131.4, 128.4, 127.1, 126.9, 114.6, 55.6, 15.9. MS (MALDI-TOF): calculated for C₁₈H₁₅NO₃ [M]⁺ 293.1052, found 293.1060.

BMO-PC, 22% yield. ¹H NMR (400 MHz, CDCl₃) δ (ppm) 8.16 (d, 2H, *J* = 8.4 Hz), 7.77–7.72 (m, 4H), 7.68 (d, 2H, *J* = 8.4 Hz), 7.18 (s, 1H), 2.44 (s, 3H). ¹³C NMR (100 MHz, CDCl₃) δ (ppm) 167.8, 166.9, 144.6, 141.5, 133.7, 133.5, 133.0, 132.9, 130.4, 128.0, 127.8, 111.9, 23.6, 16.0. MS (MALDI-TOF): calculated for C₁₈H₁₂N₂O₂ [M+H]⁺ 289.0972, found 289.0984.

TPE-BMO, 46% yield. ¹H NMR (400 MHz, CDCl₃) δ (ppm) 8.11 (d, 2H, *J* = 8.4 Hz), 7.63 (d, 2H, *J* = 8.4 Hz), 7.40 (d, 2H, *J* = 6.8 Hz), 7.16 (s, 1H), 7.14–7.02 (m, 17H), 2.42 (s, 3H). ¹³C NMR (100 MHz, CDCl₃) δ (ppm) 168.1, 166.1, 144.0, 143.8, 143.4, 141.7, 140.5, 137.7, 132.9, 132.5, 132.2, 131.6, 131.3, 128.0, 127.9, 127.4, 126.8, 126.7, 126.4, 15.9. MS (MALDI-TOF) calculated for C₃₇H₂₇NO₂ [M+H]⁺ 518.2115, found 518.2120.

TPA-BMO, 53% yield. ¹H NMR (400 MHz, CDCl₃) δ (ppm) 8.12 (d, 2H, *J* = 8.4 Hz), 7.65 (d, 2H, *J* = 8.4 Hz), 7.51 (d, 2H, *J* = 8.4 Hz), 7.30–7.25 (m, 4H), 7.17–7.12 (m, 7H), 7.08–7.04 (m, 2H), 2.41 (s, 3H). ¹H NMR (400 MHz, CD₂Cl₂) δ (ppm) 8.15 (d, 2H, *J* = 8.0 Hz), 7.68 (d, 2H, *J* = 8.4 Hz), 7.55 (d, 2H, *J* = 8.4 Hz), 7.31–7.28 (m, 4H), 7.14–7.05 (m, 9H), 2.40 (s, 3H). ¹³C NMR (100 MHz, CD₂Cl₂) δ (ppm) 168.4, 166.6, 148.7, 148.0, 143.7, 133.7, 133.3, 132.9, 132.3, 131.1, 129.9, 128.3, 127.2, 125.3, 123.9, 123.7, 16.0. MS (MALDI-TOF) calculated for C₂₉H₂₂N₂O₂ [M+H]⁺ 431.1754, found 431.1775.

Some of phenylaldehydes were synthesized by Suzuki coupling reaction (Scheme S1). Using TPA-PA as an example, briefly, 4-bromo-N, N-diphenylaniline (1.29 g, 4 mmol), (4-formylphenyl)boronic acid (0.66 g, 4.4 mmol), Pd(PPh₃)₄ (140 mg), K₂CO₃ (1.38 g, 10 mmol) in 50 mL of THF/water (4:1, v/v) were refluxed overnight under nitrogen. After cooling to room temperature, water was added and the mixture was extracted with dichloromethane. After removed the solvent, the crude product was further purified with silica gel column.

4'-Formyl-[1,1'-biphenyl]-4-carbonitrile, white solid, 100% yield. ¹H NMR (400 MHz, CDCl₃) δ (ppm) 10.09 (s, 1H), 8.01 (d, 2H, *J* = 8.4 Hz), 7.80–7.73 (m, 6H). ¹³C NMR (100 MHz, CDCl₃) δ (ppm) 191.8, 145.1, 144.3, 136.3, 133.0, 130.6, 128.2, 128.1, 118.8, 112.3. MS (MALDI-TOF): calculated for C₁₄H₉NO [M]⁺ 207.0684, found 207.0682.

4'-Methoxy-[1,1'-biphenyl]-4-carbaldehyde, white solid, 89% yield. ^1H NMR (400 MHz, CDCl_3) δ (ppm) 10.03 (s, 1H), 7.92 (d, 2H, $J = 8.4$ Hz), 7.71 (d, 2H, $J = 8.4$ Hz), 7.59 (d, 2H, $J = 6.8$ Hz), 7.01 (d, 2H, $J = 6.8$ Hz), 3.87 (s, 3H). ^{13}C NMR (100 MHz, CDCl_3) δ (ppm) 192.1, 160.3, 147.0, 134.9, 132.2, 130.5, 128.7, 127.3, 114.7, 55.6. MS (MALDI-TOF): calculated for $\text{C}_{14}\text{H}_{12}\text{O}_2$ $[\text{M}+\text{H}]^+$ 213.0910, found 213.0917.

TPE-PA, yellow solid, 97% yield. ^1H NMR (400 MHz, CDCl_3) δ (ppm) 10.02 (s, 1H), 7.90 (d, 2H, $J = 8.0$ Hz), 7.70 (d, 2H, $J = 8.4$ Hz), 7.39 (d, 2H, $J = 8.4$ Hz), 7.14–7.02 (m, 17H). ^{13}C NMR (100 MHz, CDCl_3) δ (ppm) 192.1, 146.9, 144.4, 143.8, 143.7, 141.9, 140.4, 137.5, 135.2, 132.2, 131.6, 131.5, 130.4, 128.0, 127.9, 127.6, 126.9, 126.8, 126.7. MS (MALDI-TOF): calculated for $\text{C}_{33}\text{H}_{24}\text{O}$ $[\text{M}+\text{H}]^+$ 437.1900, found 437.1910.

TPA-PA, yellow solid, 75% yield. ^1H NMR (400 MHz, CDCl_3) δ (ppm) 10.02 (s, 1H), 7.92 (d, 2H, $J = 8.4$ Hz), 7.72 (d, 2H, $J = 8.0$ Hz), 7.51 (d, 2H, $J = 8.0$ Hz), 7.31–7.27 (m, 4H), 7.15–7.13 (m, 6H), 7.08–7.05 (m, 2H). ^{13}C NMR (100 MHz, CDCl_3) δ (ppm) 192.1, 148.6, 147.5, 146.8, 134.9, 133.0, 130.5, 129.6, 128.2, 127.1, 125.1, 123.7, 123.3. MS (MALDI-TOF): calculated for $\text{C}_{25}\text{H}_{19}\text{NO}$ $[\text{M}+\text{H}]^+$ 350.1539, found 350.1541.

NMR spectra and HRMS of BMOs

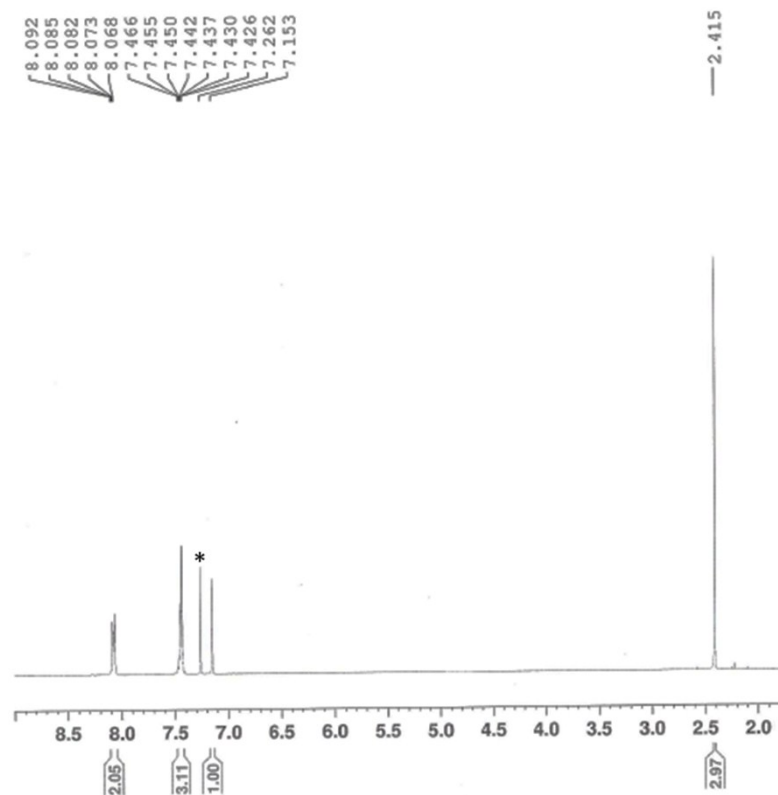


Fig. S1 ^1H NMR spectra of BMO-H in CDCl_3 . The solvent peak was marked with asterisk.

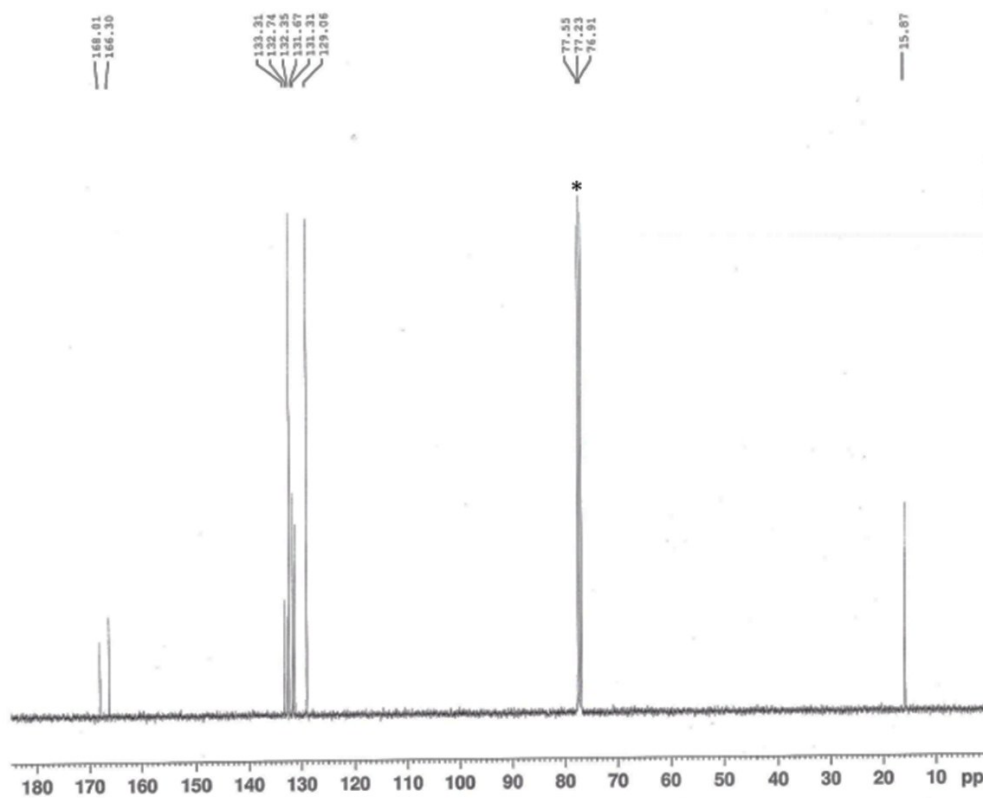


Fig. S2 ^{13}C NMR spectra of BMO-H in CDCl_3 . The solvent peak was marked with asterisk.

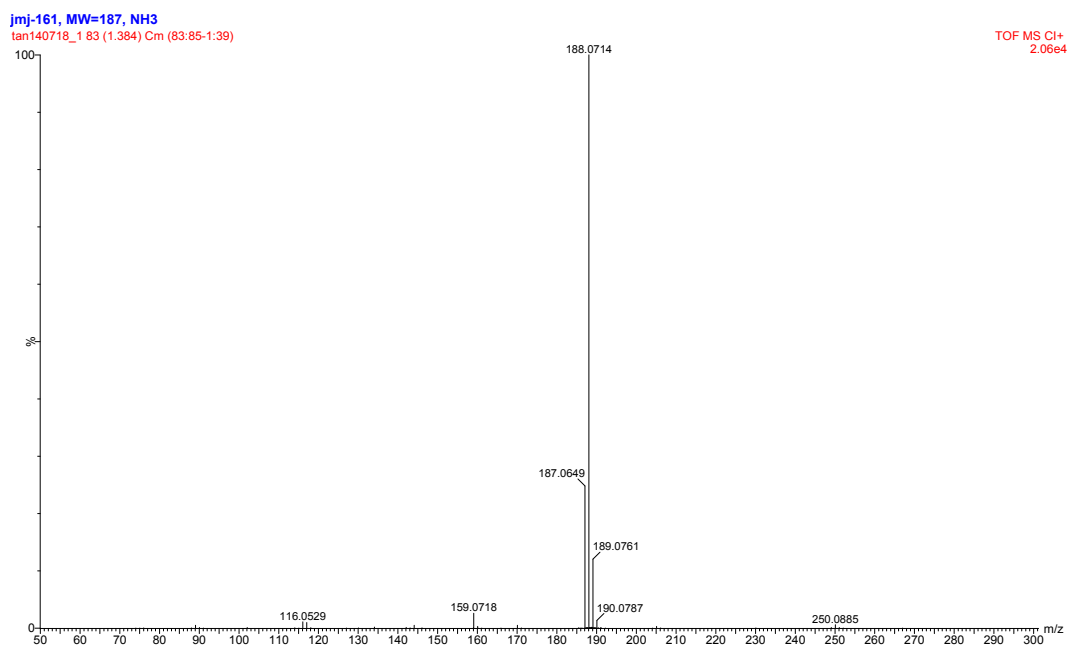


Fig. S3 HRMS spectra of BMO-H.

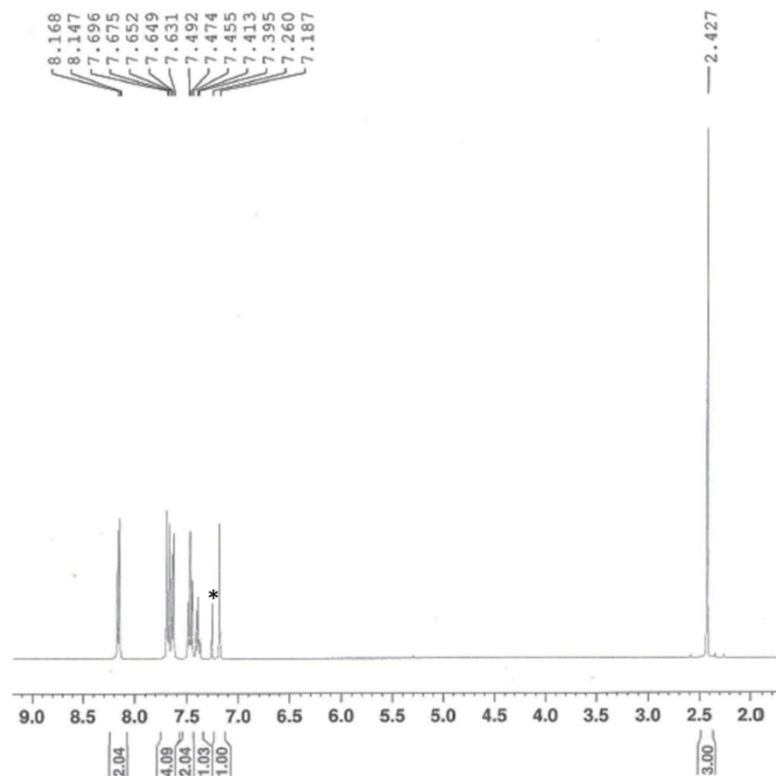


Fig. S4 ^1H NMR spectra of BMO-PH in CDCl_3 . The solvent peak was marked with asterisk.

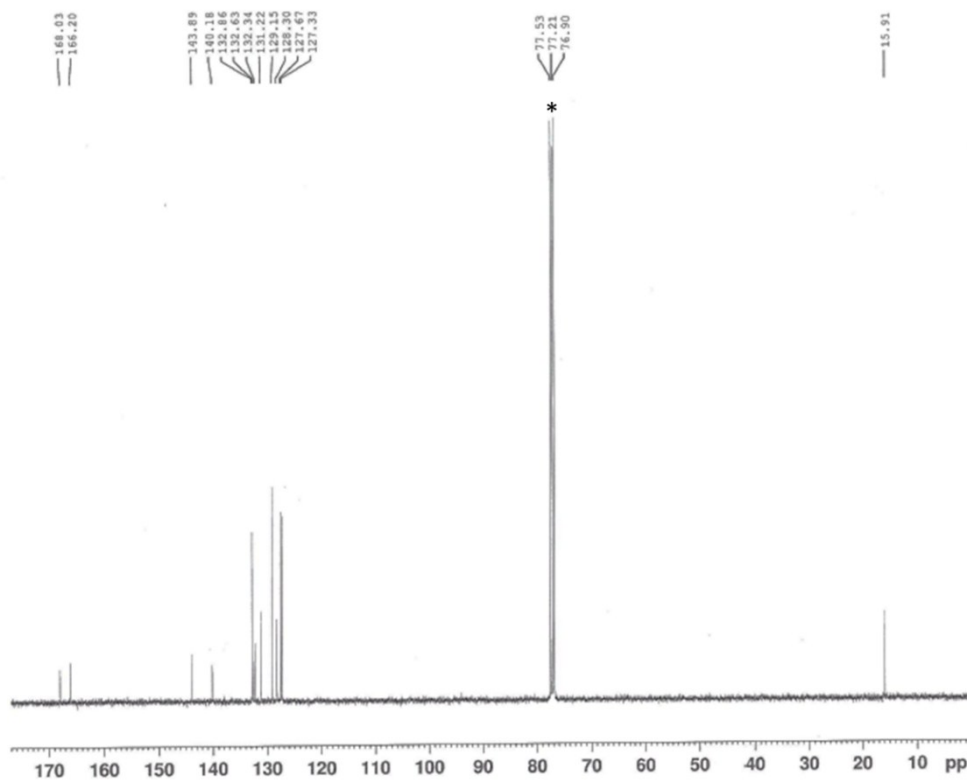


Fig. S5 ^{13}C NMR spectra of BMO-PH in CDCl_3 . The solvent peak was marked with

asterisk.

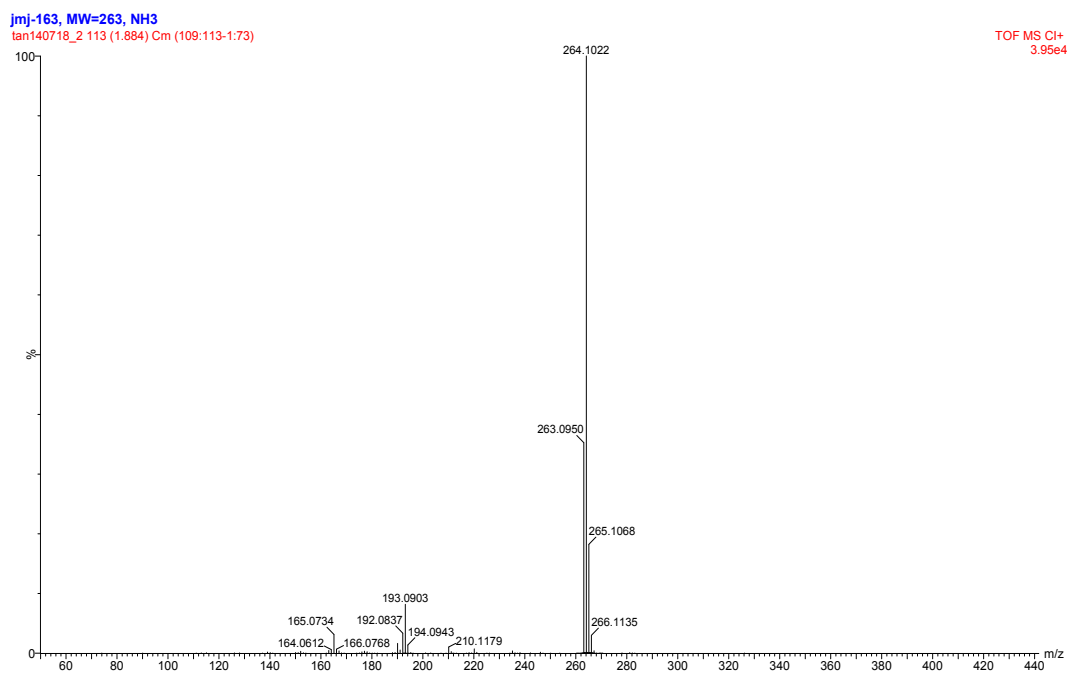


Fig. S6 HRMS spectra of BMO-PH.

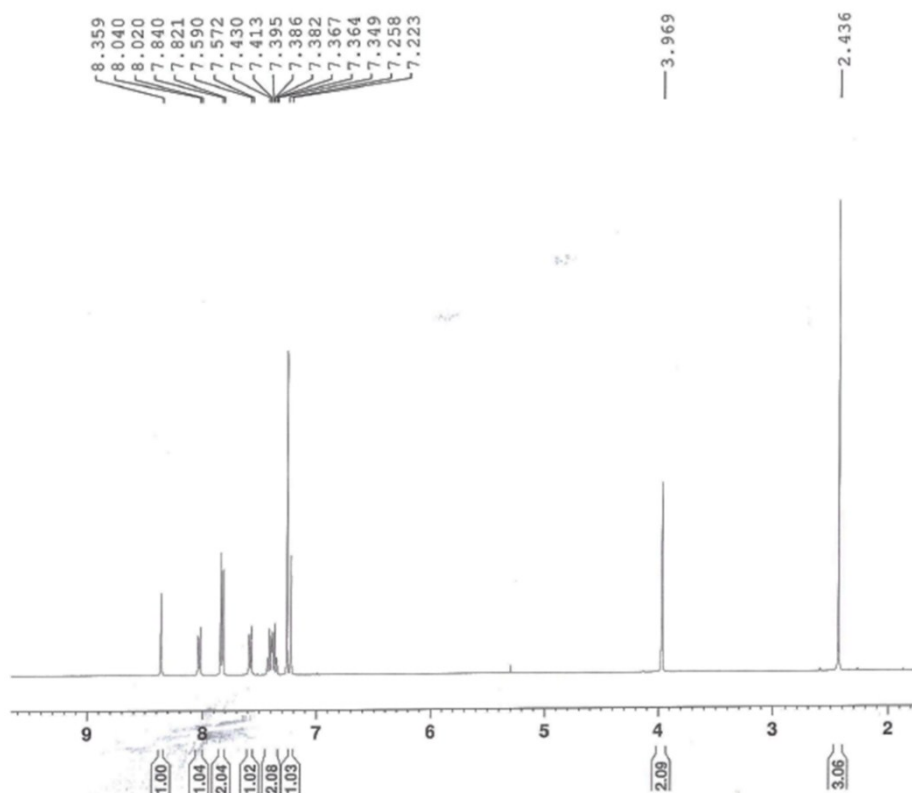


Fig. S7 ¹H NMR spectra of BMO-PF in CDCl₃. The solvent peak was marked with asterisk.

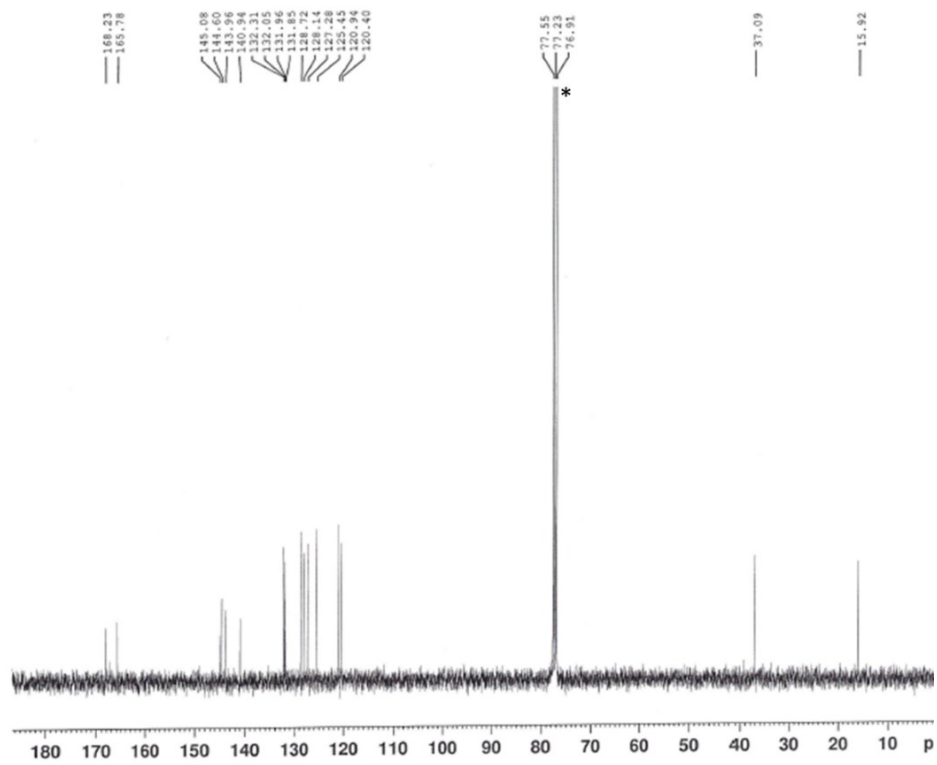


Fig. S8 ^{13}C NMR spectra of BMO-PF in CDCl_3 . The solvent peak was marked with asterisk.

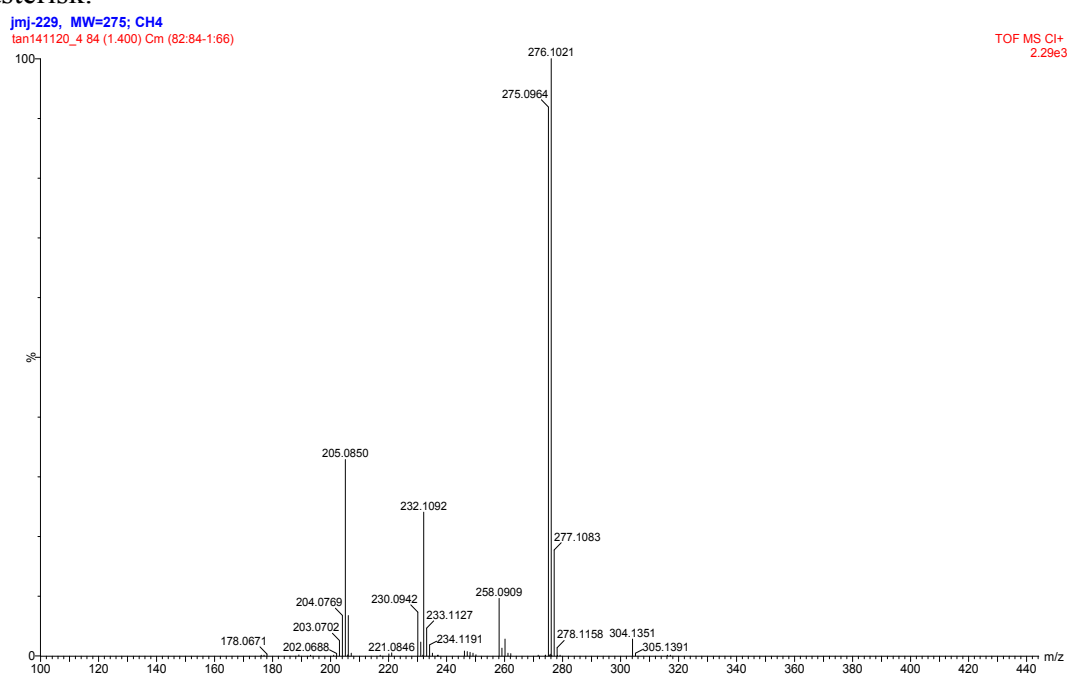


Fig. S9 HRMS spectra of BMO-PF.

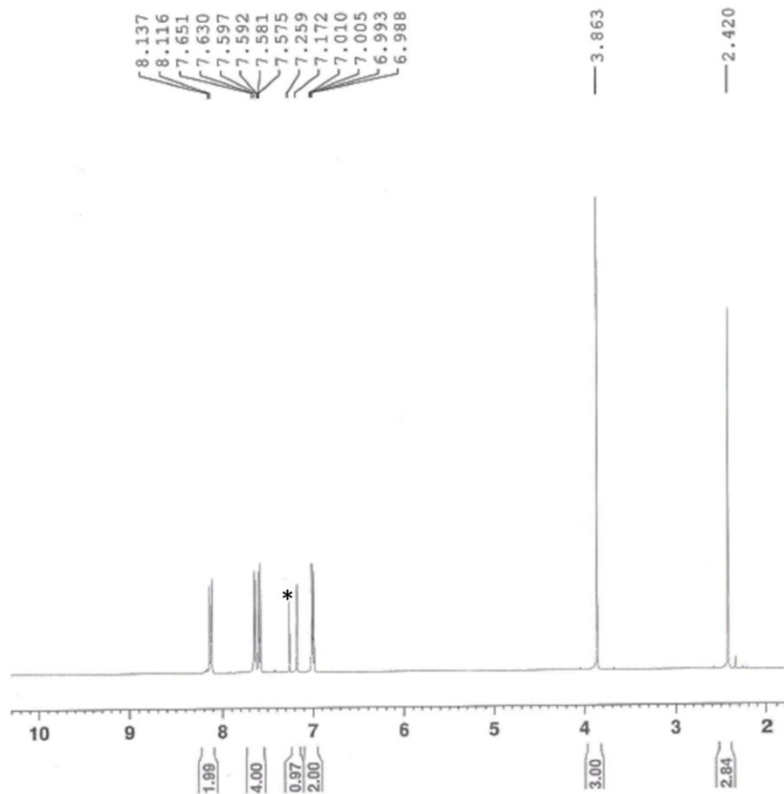


Fig. S10 ^1H NMR spectra of BMO-PM in CDCl_3 . The solvent peak was marked with asterisk.

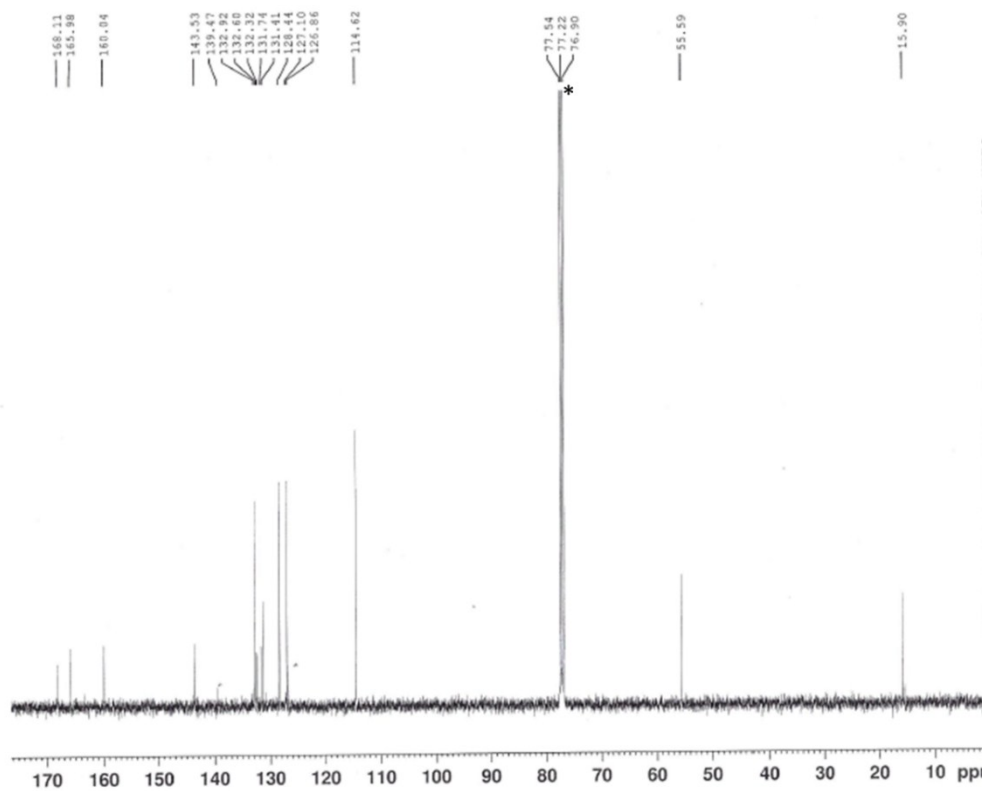


Fig. S11 ^{13}C NMR spectra of BMO-PM in CDCl_3 . The solvent peak was marked with

asterisk.

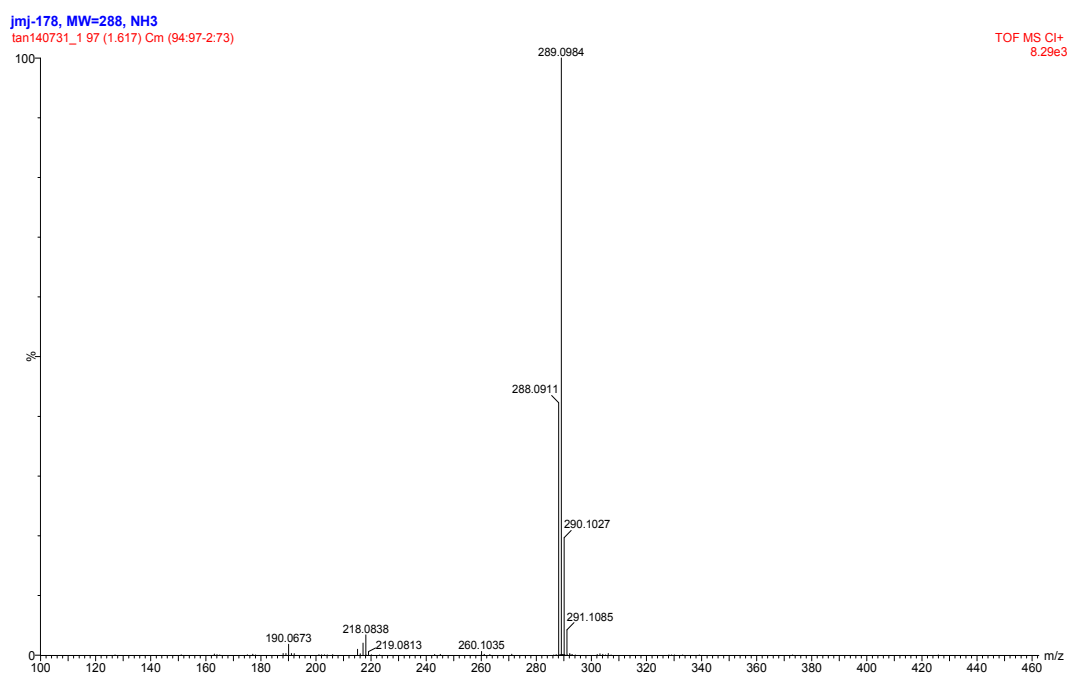


Fig. S12 HRMS spectra of BMO-PM.

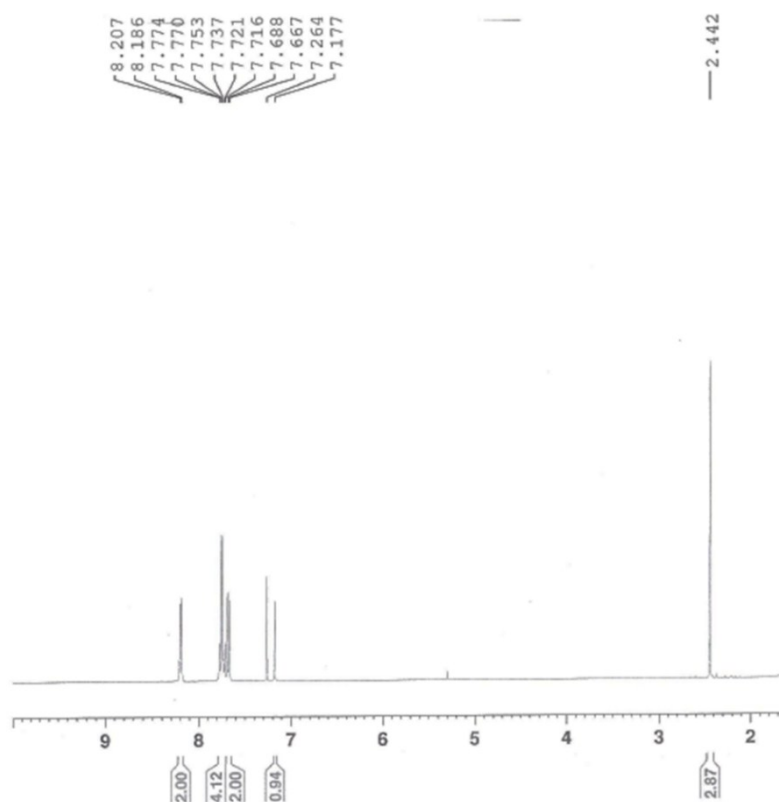


Fig. S13 ¹H NMR spectra of BMO-PC in CDCl₃. The solvent peak was marked with asterisk.

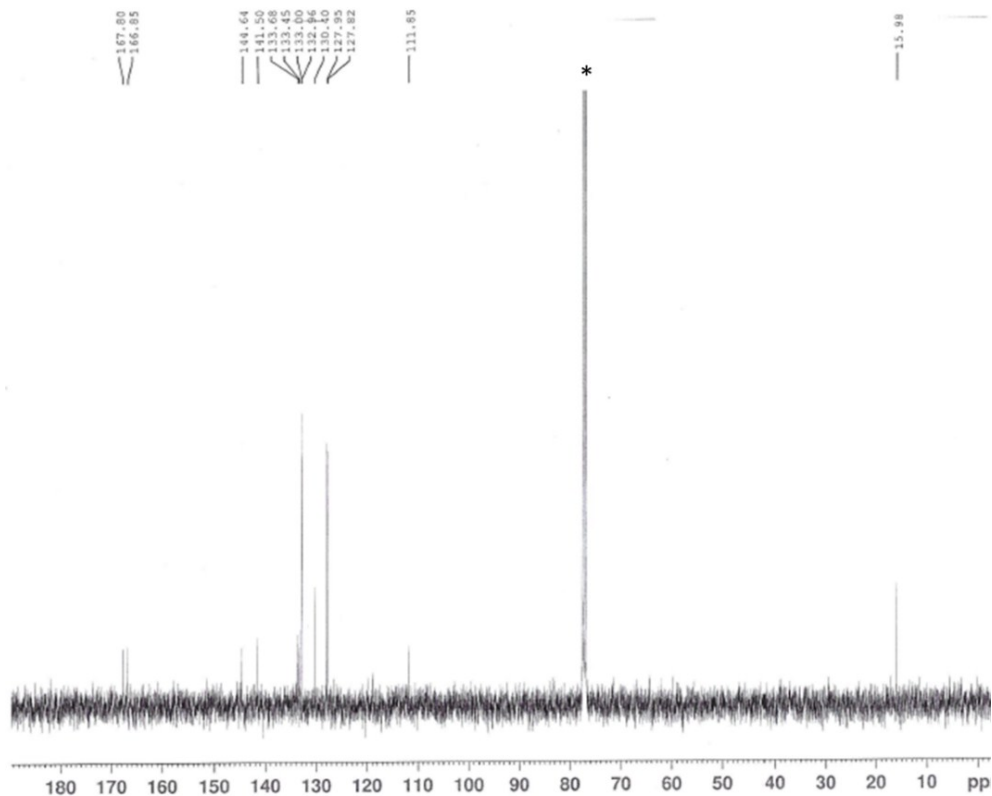


Fig. S14 ^{13}C NMR spectra of BMO-PC in CDCl_3 . The solvent peak was marked with asterisk.

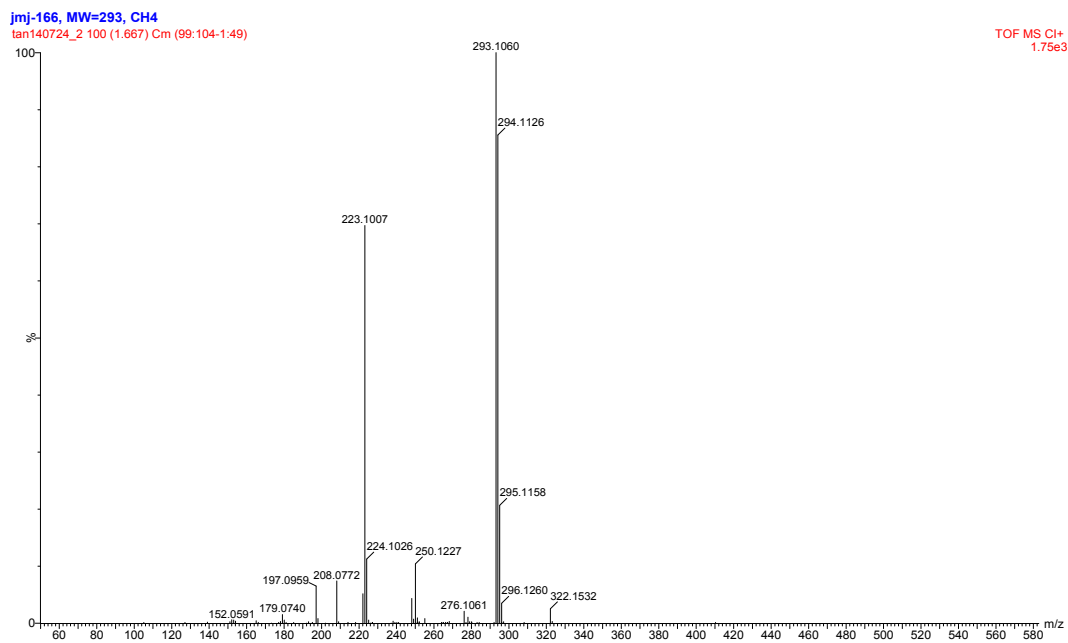


Fig. S15 HRMS spectra of BMO-PC.

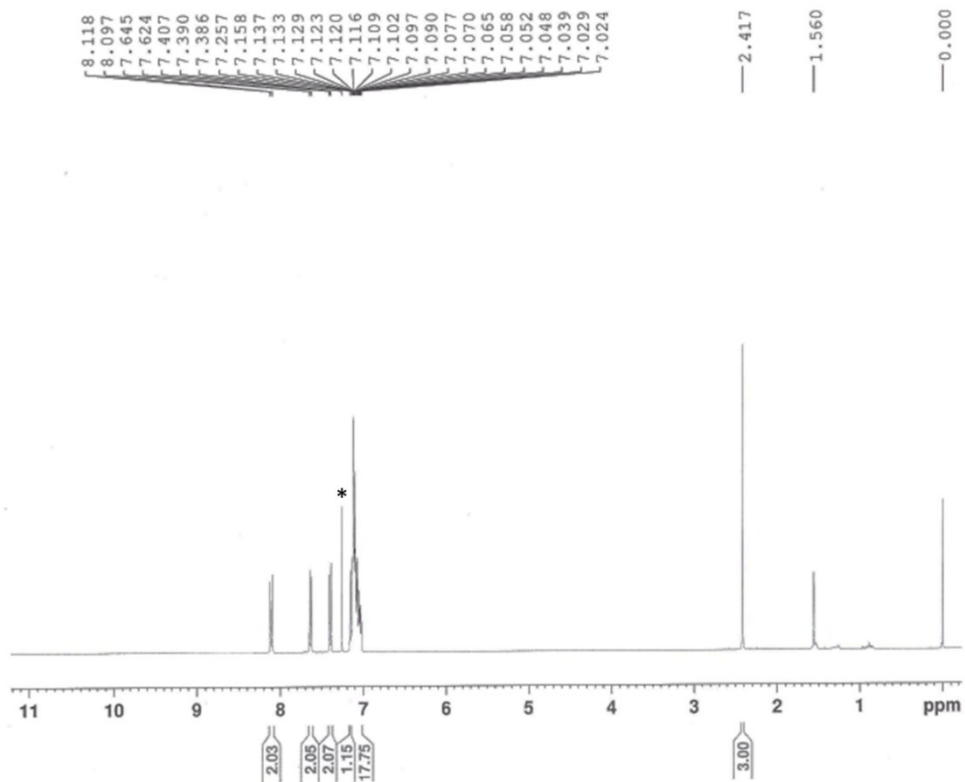


Fig. S16 ^1H NMR spectra of TPE-BMO in CDCl_3 . The solvent peak was marked with asterisk.

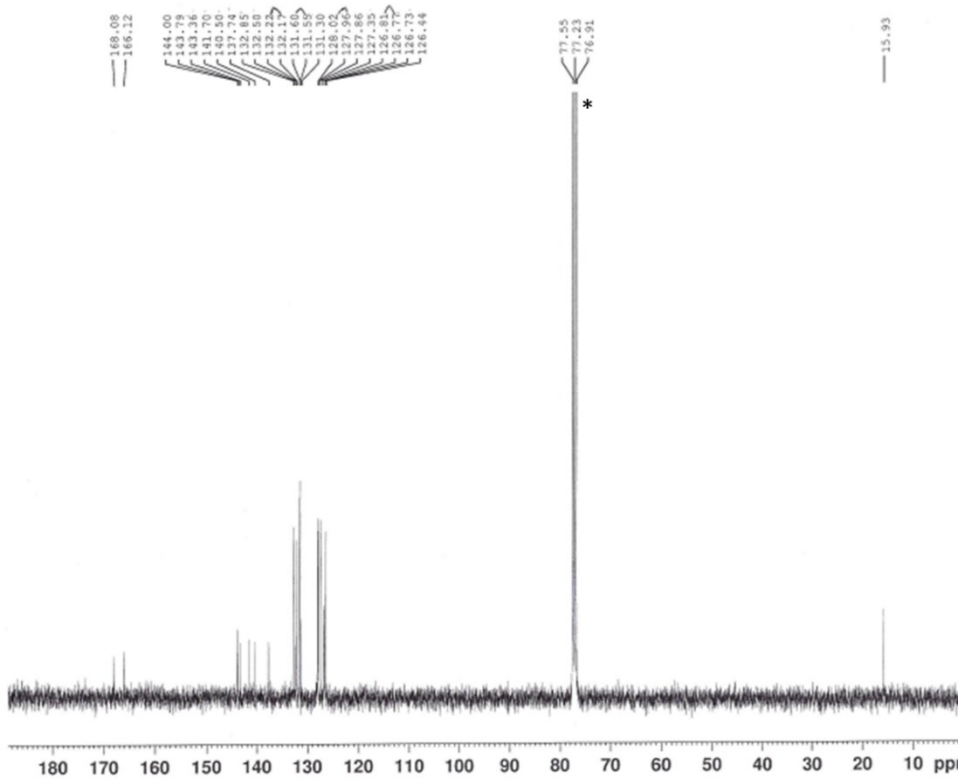


Fig. S17 ^{13}C NMR spectra of TPE-BMO in CDCl_3 . The solvent peak was marked with asterisk.

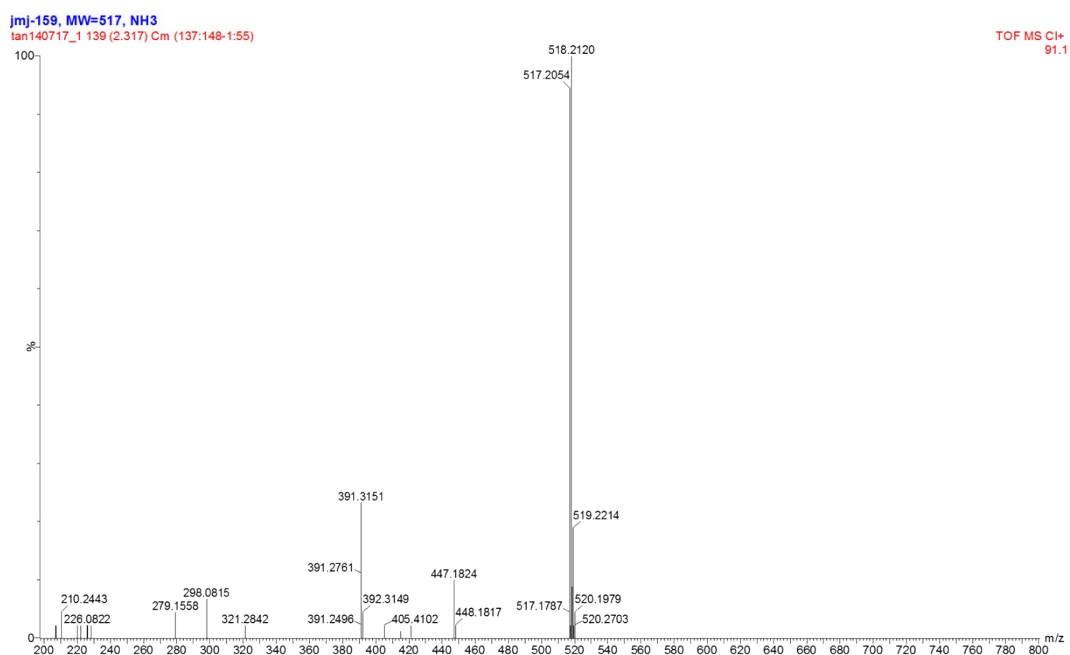


Fig. S18 HRMS spectra of TPE-BMO.

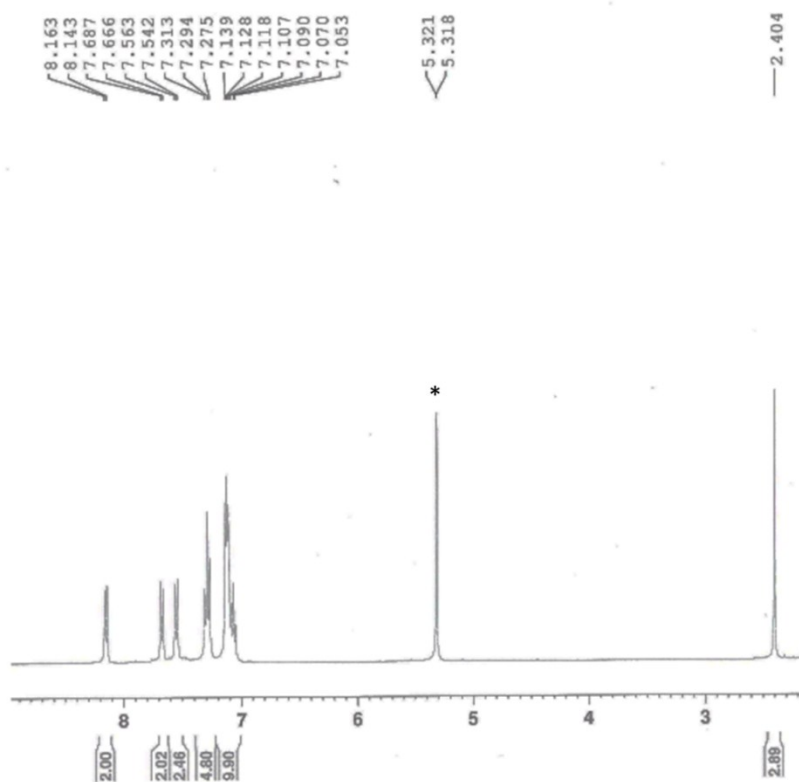


Fig. S19 ^1H NMR spectra of TPA-BMO in CD_2Cl_2 . The solvent peak was marked with asterisk.

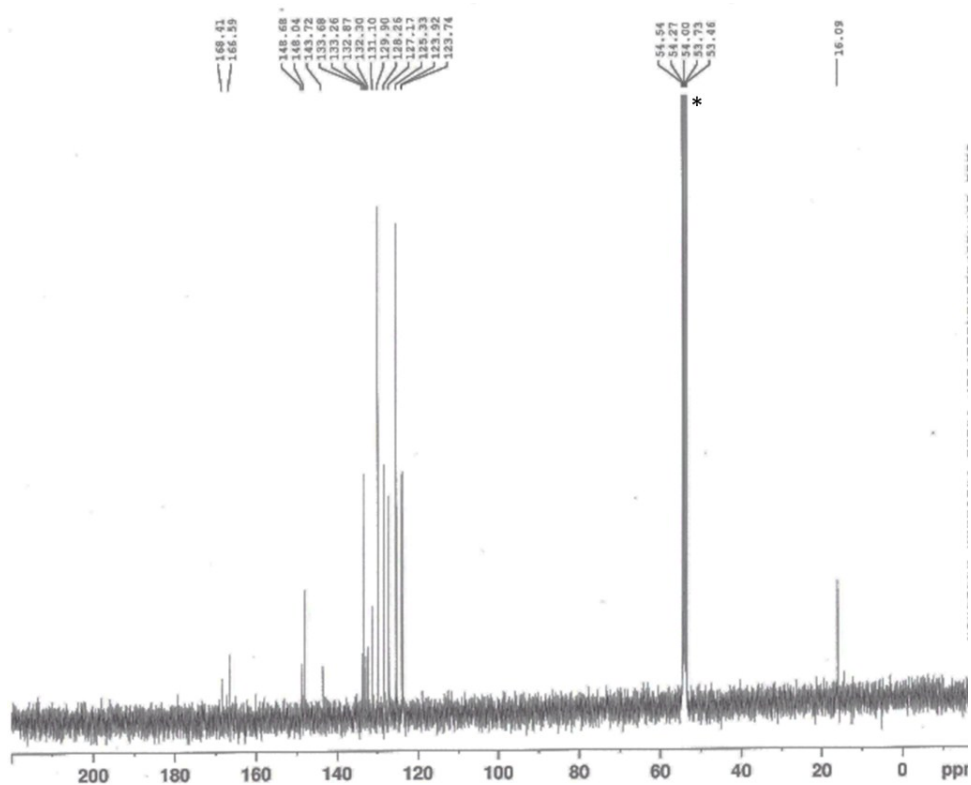


Fig. S20 ^{13}C NMR spectra of TPA-BMO in CD_2Cl_2 . The solvent peak was marked with asterisk.

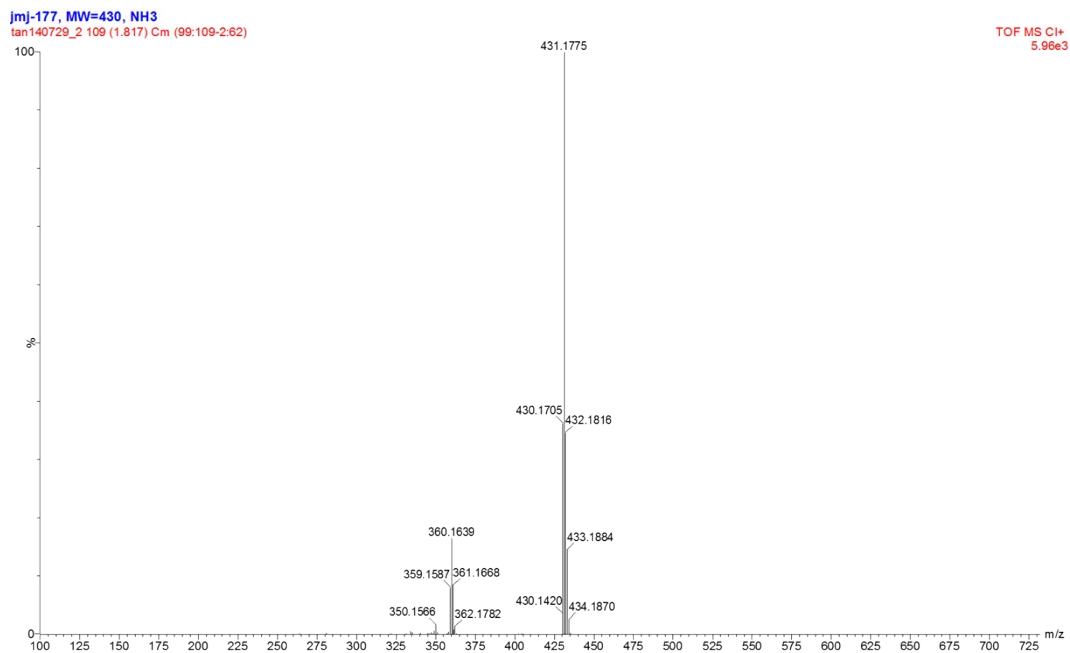


Fig. S21 HRMS spectra of TPA-BMO.

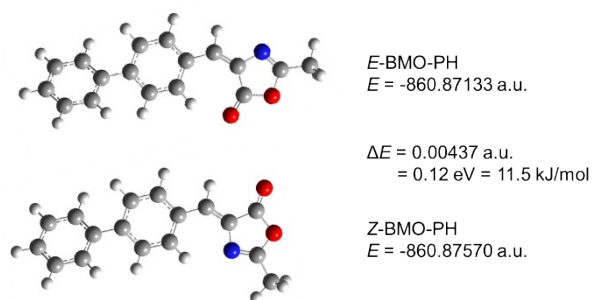


Fig. S22 Optimized structure of E -BMO-PH and Z -BMO-PH.

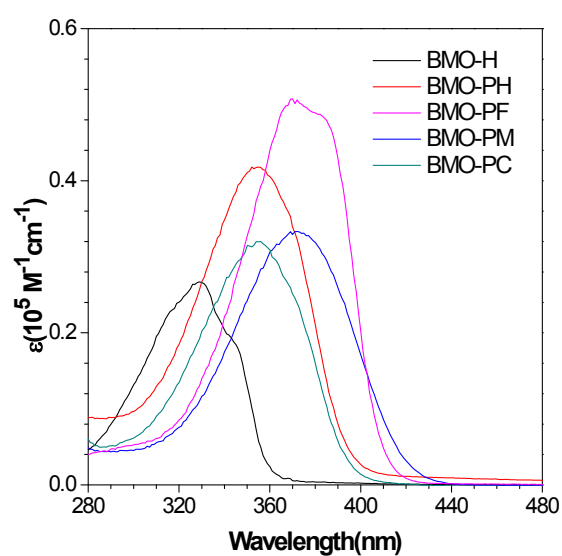


Fig. S23 UV-Vis absorption of BMOs in THF. Dye concentration = 10 μ M.

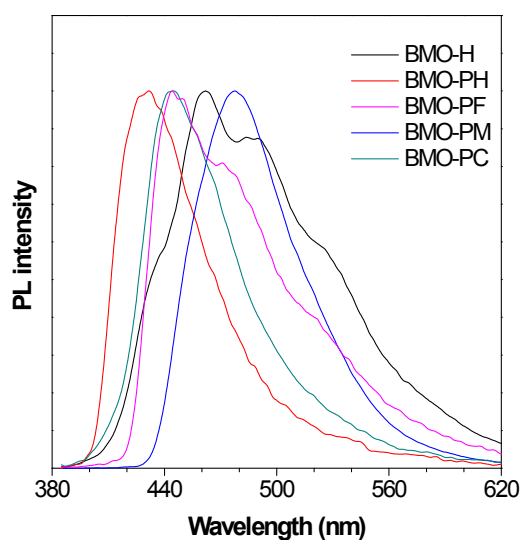


Fig. S24 Fluorescent emission spectra of BMOs in THF. Excitation wavelength = 365 nm. Dye concentration = 20 μ M.

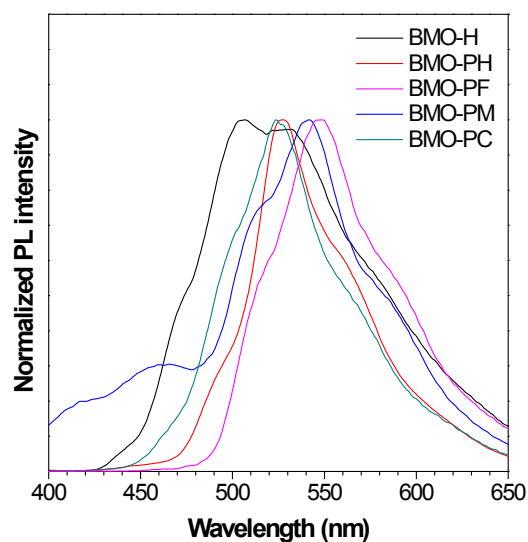


Fig. S25 Fluorescent emission spectra of BMOs in solid state. Excitation wavelength = 365 nm.

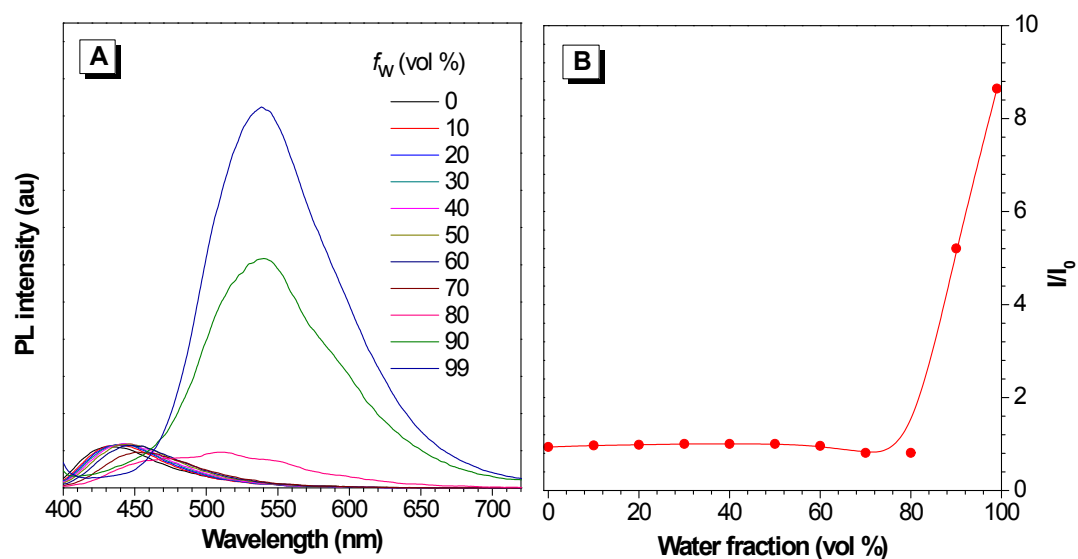


Fig. S26 (A) Emission spectra and (B) AIE plot of relative peak intensity of BMO-PF at the concentration of 10 μM in THF-water mixtures with increasing water fractions (f_w). I_0 is the peak intensity of THF solution. Excitation wavelength = 380 nm.

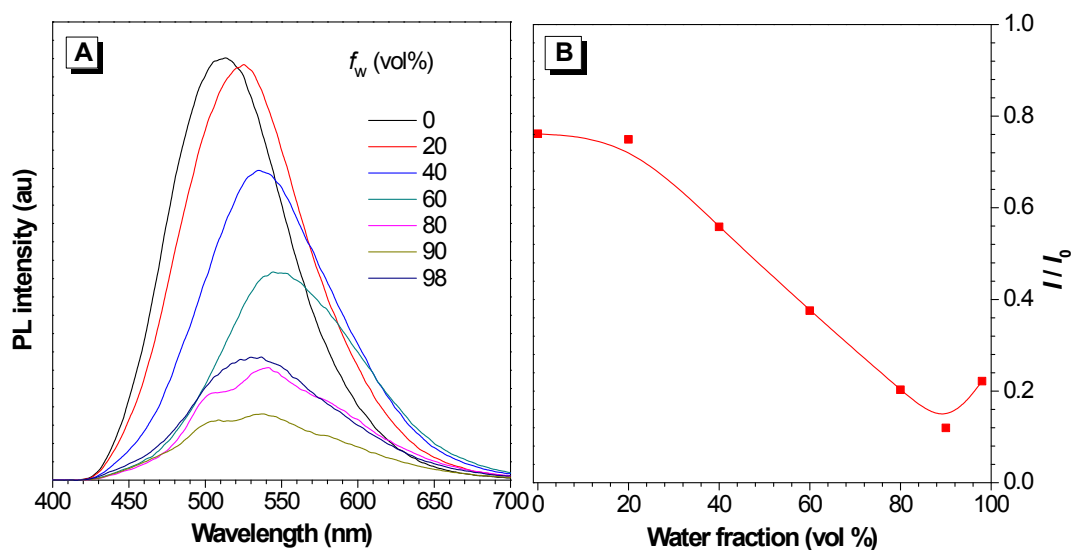


Fig. S27 (A) Emission spectra and (B) AIE plot of relative peak intensity of BMO-PM at the concentration of $20 \mu\text{M}$ in DMSO-water mixtures with increasing water fractions (f_w). I_0 is the peak intensity of DMSO solution. Excitation wavelength = 365nm .

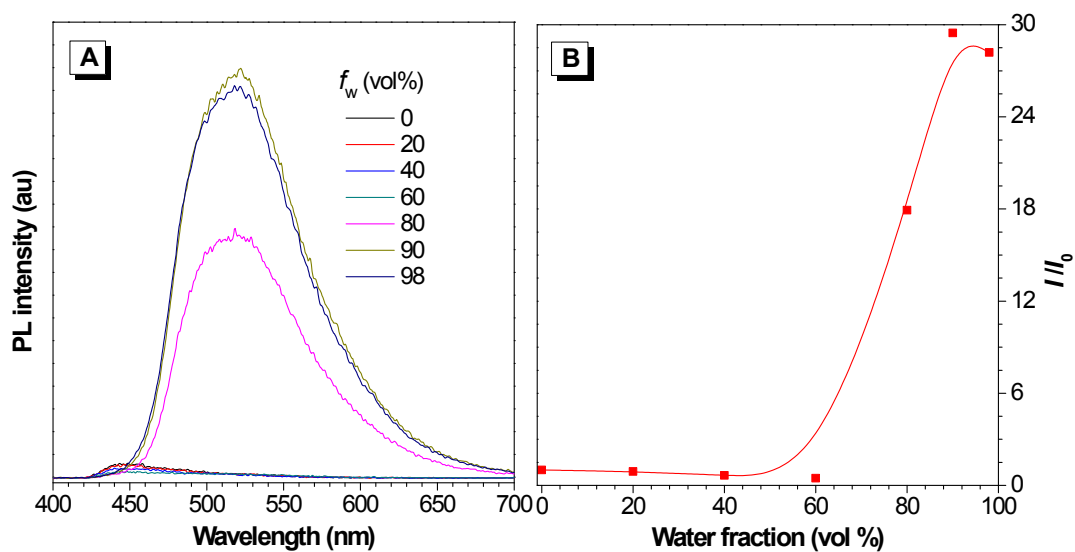


Fig. S28 (A) Emission spectra and (B) AIE plot of relative peak intensity of BMO-PC at the concentration of $20 \mu\text{M}$ in DMSO-water mixtures with increasing water fractions (f_w). I_0 is the peak intensity of DMSO solution. Excitation wavelength = 365nm .

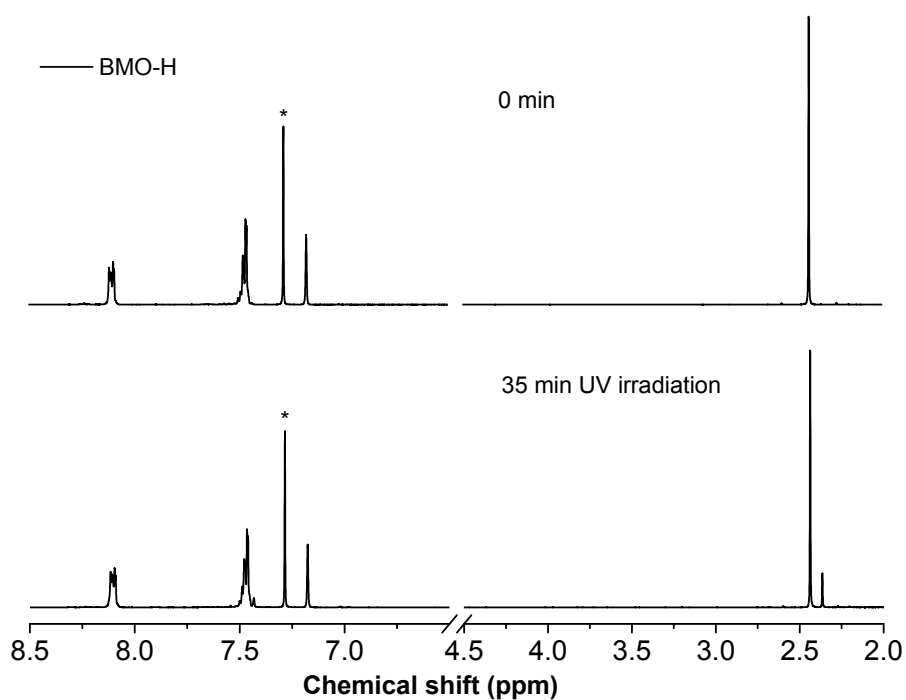


Fig. S29 *E/Z* photoisomerization process is monitored by ¹H NMR spectra. Starting from a 100% *Z* isomer (0 min, upper spectra), BMO-H in CDCl₃ (40 mM) was irradiated by a UV lamp for 35min (lower spectra). Solvent (CHCl₃) peak was marked with asterisk.

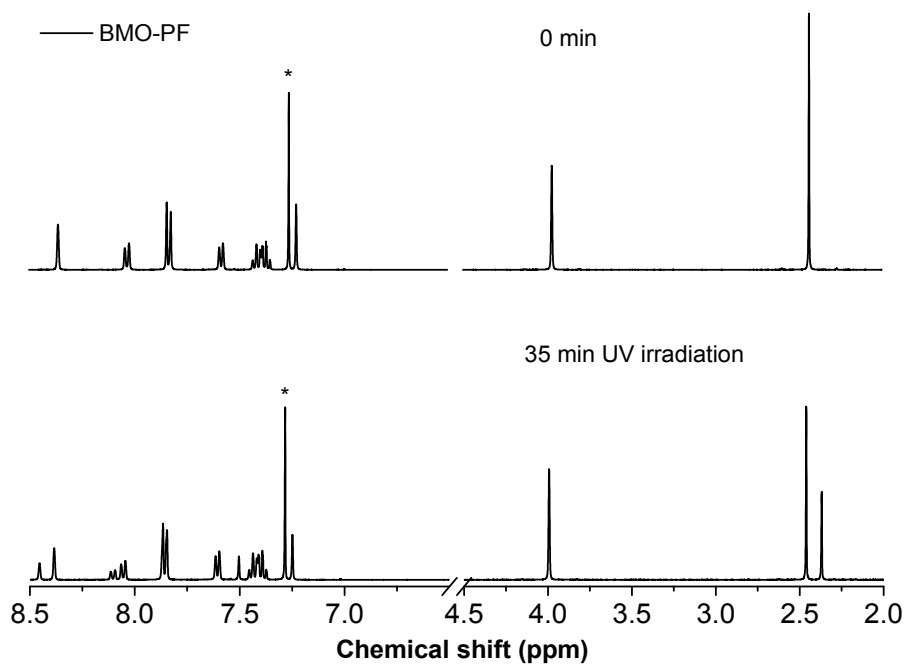


Fig. S30 *E/Z* photoisomerization process is monitored by ¹H NMR spectra. Starting from a 100% *Z* isomer (0 min, upper spectra), BMO-PF in CDCl₃ (40

mM) was irradiated by a UV lamp for 35min (lower spectra). Solvent (CHCl_3) peak was marked with asterisk.

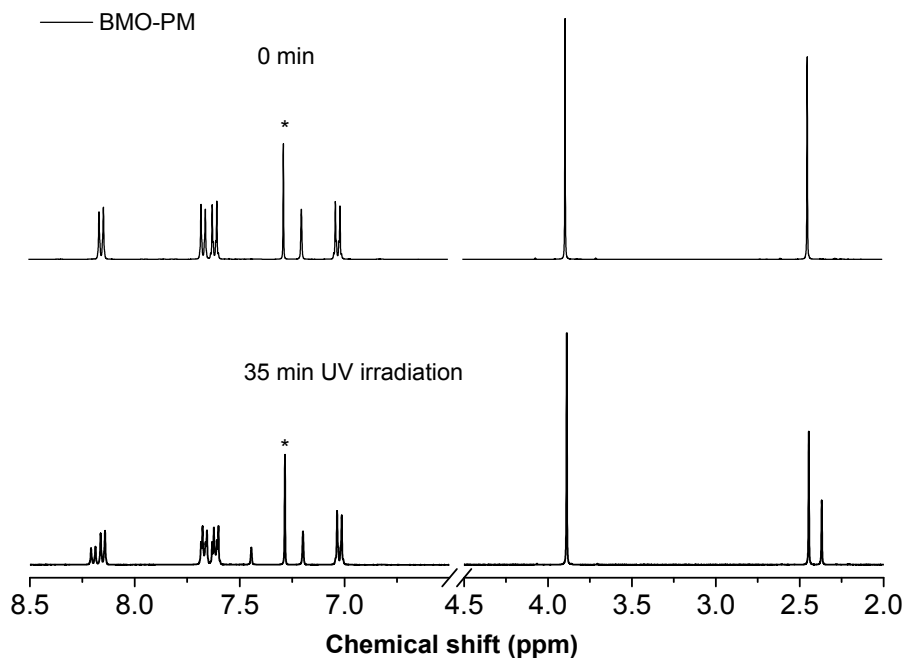


Fig. S31 *E/Z* photoisomerization process is monitored by ^1H NMR spectra. Starting from a 100% *Z* isomer (0 min, upper spectra), BMO-PM in CDCl_3 (40 mM) was irradiated by a UV lamp for 35min (lower spectra). Solvent (CHCl_3) peak was marked with asterisk.

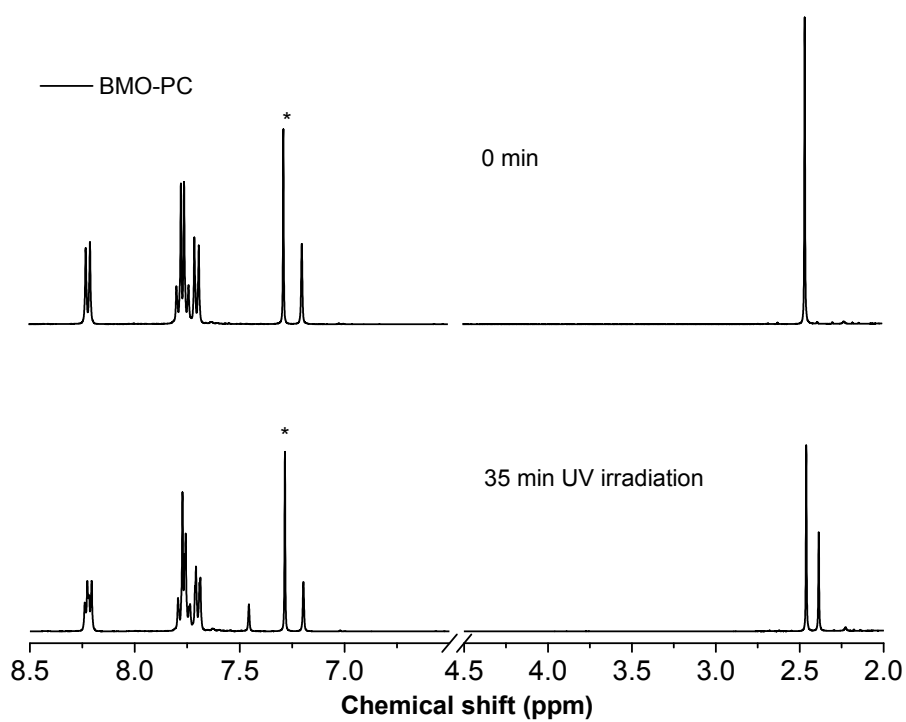


Fig. S32 *E/Z* photoisomerization process is monitored by ^1H NMR spectra. Starting from a 100% *Z* isomer (0 min, upper spectra), BMO-PC in CDCl_3 (40 mM) was irradiated by a UV lamp for 35min (lower spectra). Solvent (CHCl_3) peak was marked with asterisk.

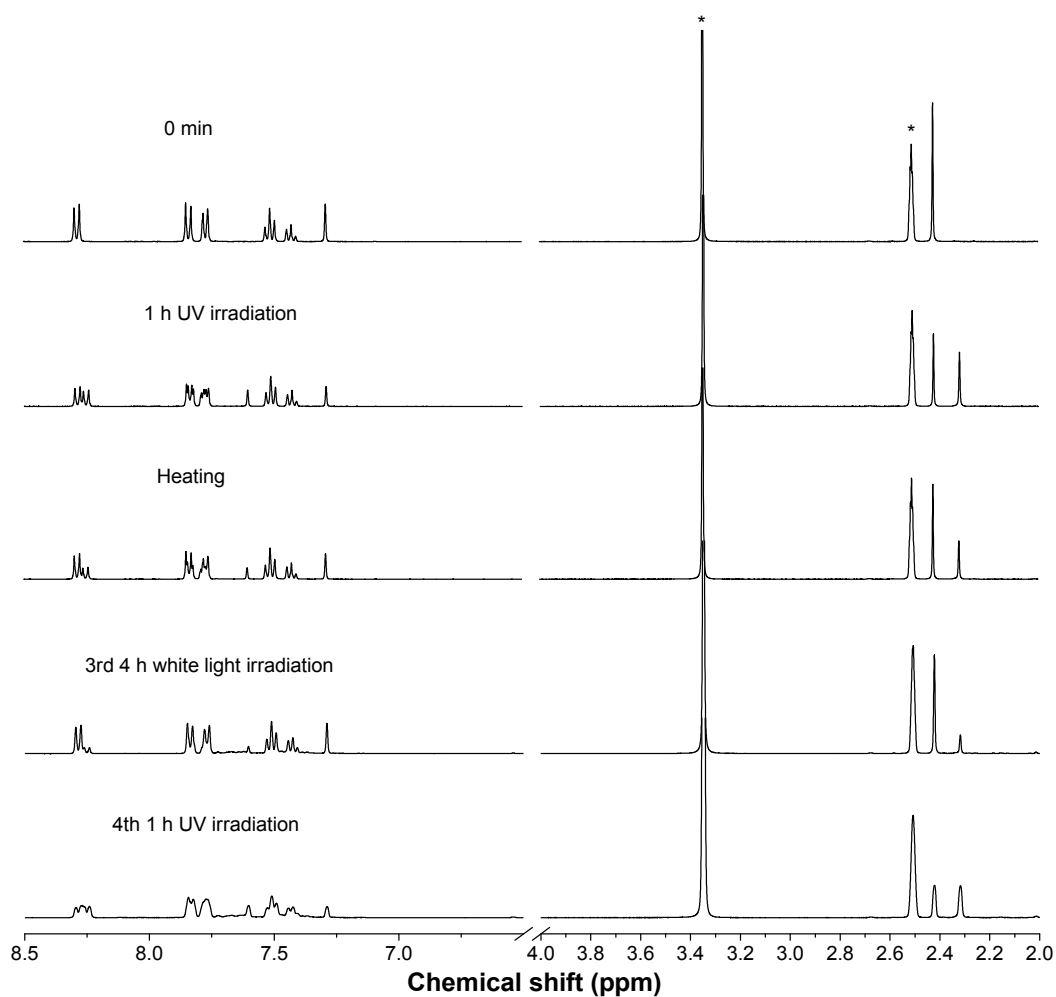


Fig. S33 ^1H NMR spectra of BMO-PH (d_6 -DMSO, 20 m) after heating and UV/white light irradiation. Solvent peaks were marked with asterisks.

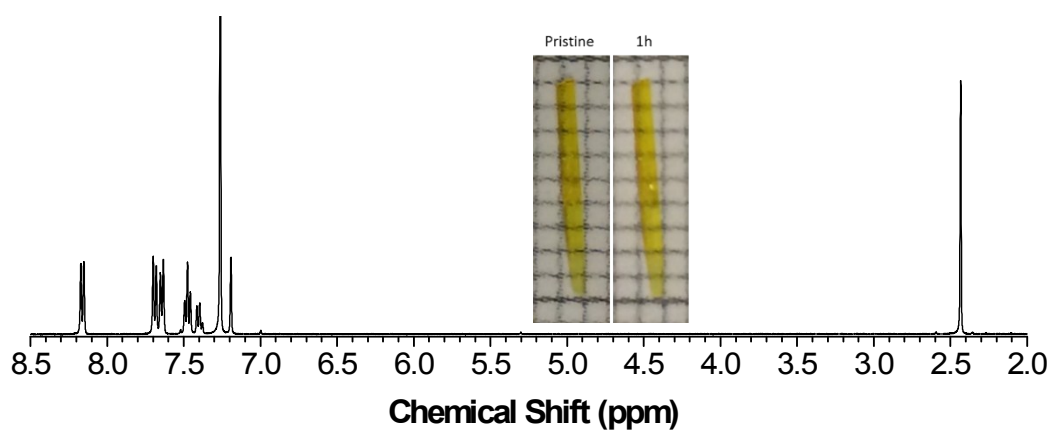


Fig. S34 ^1H NMR spectra in CDCl_3 of the crystal BMO-PH after 365-nm irradiation for 1h. The scale of inset photo is 0.9 mm*0.9 mm each blog.

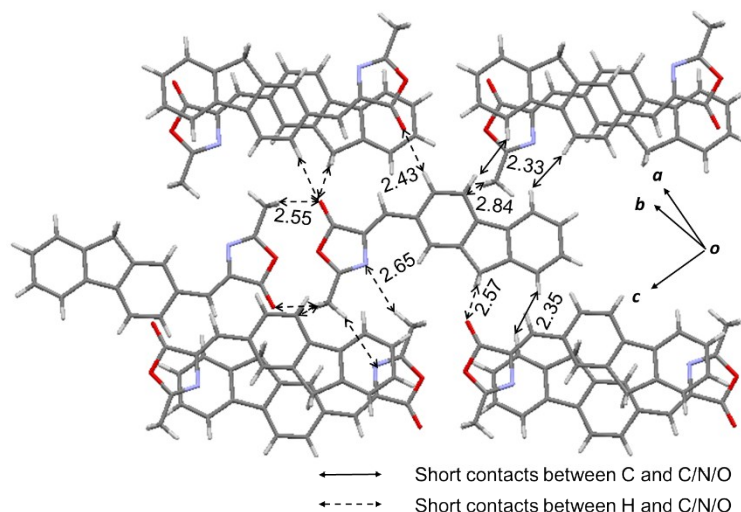


Fig. S35 Restriction of intramolecular motions of BMO-PF by neighboring molecules. Some of the short contacts are assigned and distances are noted (unit: Å).

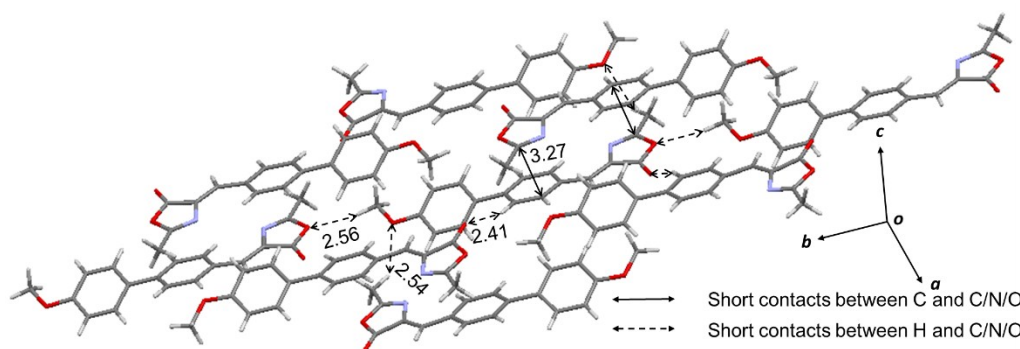


Fig. S36 Restriction of intramolecular motions of BMO-PM by neighboring molecules. Some of the short contacts are assigned and distances are noted (unit: Å).

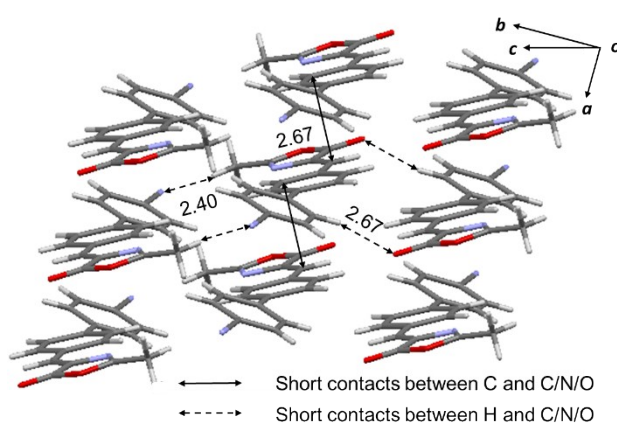


Fig. S37 Restriction of intramolecular motions of BMO-PC by neighboring molecules. Some of the short contacts are assigned and distances are noted (unit: Å).

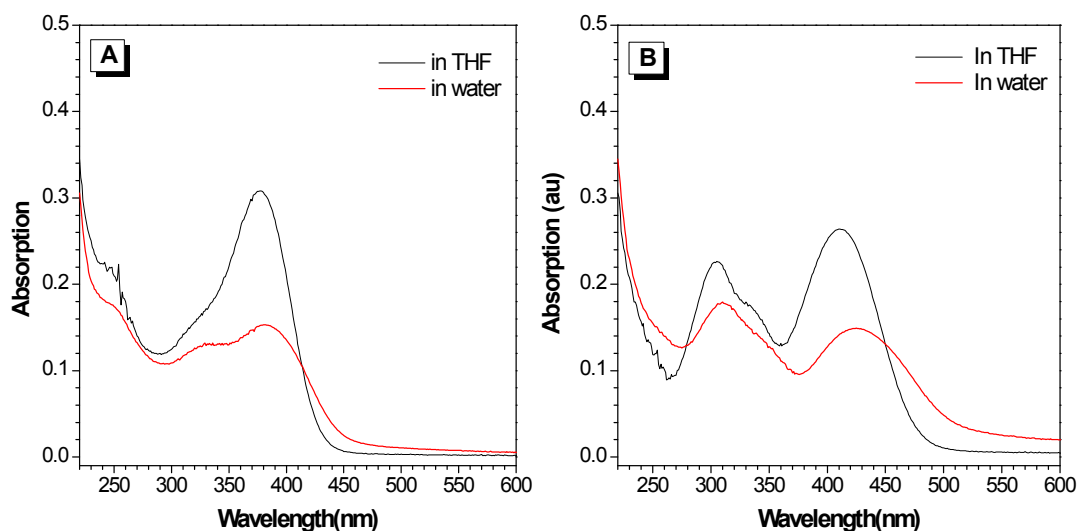


Fig. S39 UV-vis absorption of (A)TPE-BMO and (B)TPA-BMO in THF and water (containing 1 vol % THF). Dye concentration = 10 μ M.

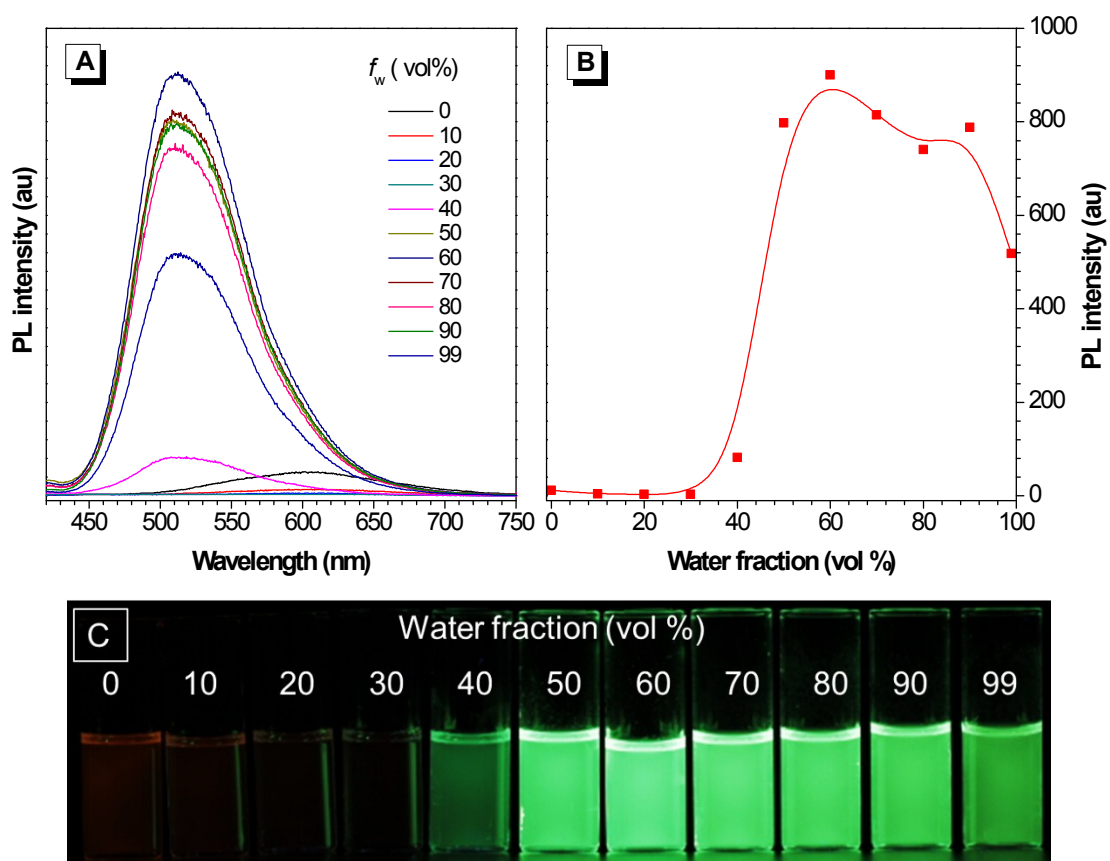


Fig. S40 (A) PL spectra and (B) plot of PL intensity at 510 nm of TPE-BMO in DMSO/water mixtures versus water fraction. Excitation wavelength = 400 nm. Dye concentration = 5 μ M.

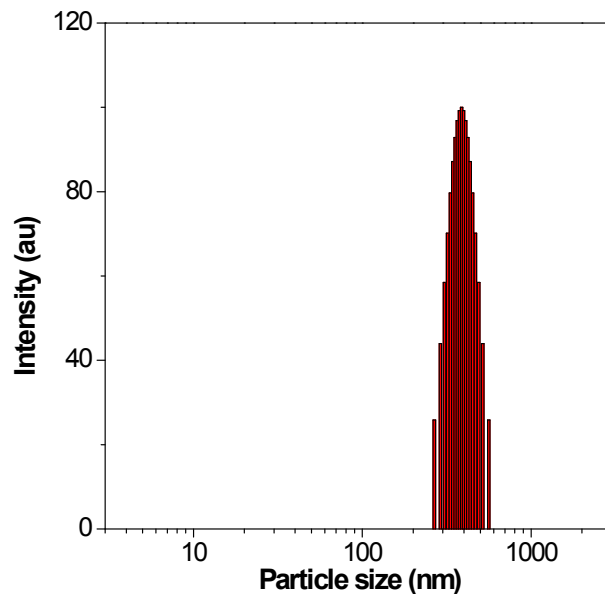


Fig. S41 Dynamic light scattering (DLS) result of aggregates of TPE-BMO in DMSO/water mixture with 70 vol % water fraction. Dye concentration = 5 μ M.

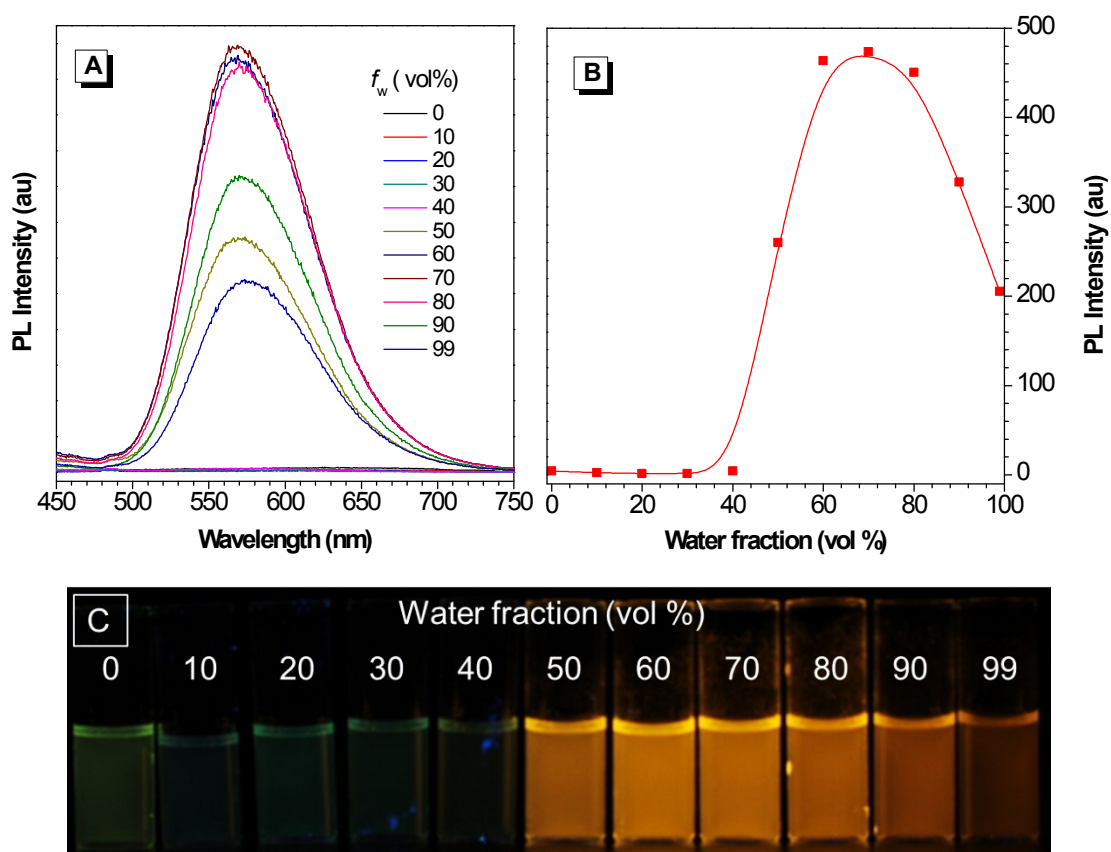


Fig. S42 (A) PL spectra and (B) plot of PL intensity at 568nm of TPA-BMO in DMSO/water mixtures versus water fraction. Excitation wavelength = 420 nm. Dye concentration = 5 μ M.

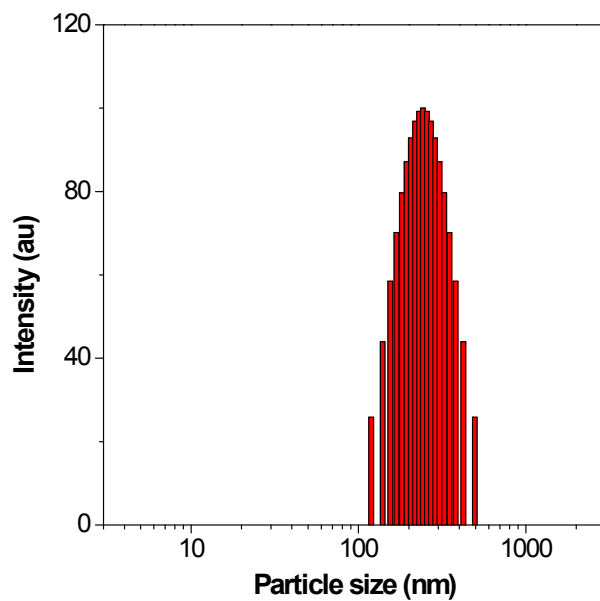


Fig. S43 DLS result of aggregates of TPA-BMO in DMSO/water mixture with 70 vol % water fraction. Dye concentration = 5 μ M.

References

1. M. Blanco-Lomas, I. Funes-Ardoiz, P. J. Campos and D. Sampedro, *Eur. J Org. Chem.*, 2013, **2013**, 6611-6618.